Multi-Dimensional Fuzzy C-Mean Considering Spatial Information for Brain MRI Segmentation

Jamal Ghasemi[1], Mohammad Reza Karami Mollaei[2], Reza Ghaderi[3], Ali Hojjatoleslami[4]
1-Faculty of Engineering & Technology, University of Mazandaran, Iran
2-Department of Electrical and Computer, Babol University of Technology, Babol, Iran
3-Shahid Beheshti University, Tehran, Iran
4-School of Computing, University of Kent, Canterbury, UK

Received July 2013 Revised September 2013 Accepted November 2013

ABSTRACT:
Due to artifacts, brain magnetic resonance image (MRI) segmentation is a complicated concern. This research work presents an image segmentation approach for brain magnetic resonance (MR) images. The proposed method is based on multi dimensional fuzzy C-mean. In this technique, different features of neighbouring pixels such as mean, standard deviation and singular value are extracted and then a multi dimensional feature vector is created in feature selection stage in which the best combination of extracted features is used. The created feature vector is used as an input to the multi dimensional FCM. The results have been evaluated with manual segmentation on two publicly available datasets.

KEYWORDS: Brain MRI, Segmentation, Fuzzy c-mean

1. INTRODUCTION

Medical images cause profound improvements in diagnosing different types of disease. One of their advantages is to assist decision making of physicians without any additional process. They provide critical information about internal organs through non invasive procedures which helps the specialists to detect abnormal changes in the tissue. Generally, investigation methods and disease diagnosis are dependent on physician experiences. In recent decades, computer-based image processing techniques cause a better perception of medical images. MRI is one of the most important techniques of medical imaging which plays a key role in brain tissue visualization. MRI is a non invasive technique which generates high resolution images of high intensity contrast for different soft tissues. Three main tissues in a normal MRI are: Gray Matter (GM), White Matter (WM) and cerebrospinal fluid (CSF). Any anomaly tissue apart from these three mentioned tissues is investigated as a medical disorder [1]. Brain MRI segmentation (BMS) is one of the important processing operations in which a special region of the image is labelled [2]. Whereas brain MRI is a set of images with large volume information, manual BMS is a time consuming task. Therefore, an automatic segmentation system with the acceptable speed, high accuracy and generalization capability is needed. There are many problems affecting BMS results which are noise, partial volume effect (PVE) and intensity non-uniformity (INU).The main sources of noise are categorized according to biological and scanner noises introduced in earlier studies [3-6].

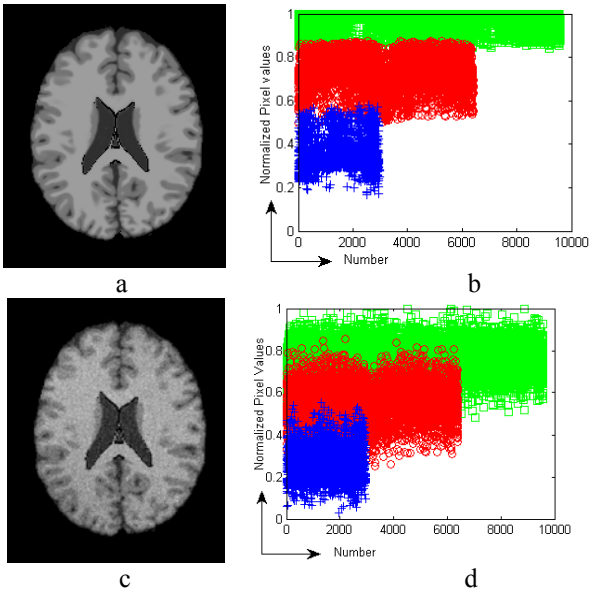

Fig. 1. Tissues overlap in Brain MRI. Blue: CSF, Red: GM and Green: WM.(a) Artifact free (ideal) brain MRI; (b) Intensity distribution of image (a); (c) Brain MRI with 9% noise and 40% INU; (d) Intensity distribution of image (c)

PVE is recognized as mixing of intensities due to more than one tissue present at the pixel.
INU, also called bias, the field is a low frequency smoothed artifact which is generated by in-homogeneity of magnetic field during scanning process [7], [8]. MRI problems lead to a pixel uncertainty which leads to a considerable overlap between different tissues [9]. This is shown in Fig. 1.
Ideally, in a set of MRI, the pixel intensity of each tissue should be constant or has a Gaussian distribution with low standard deviation considering PVE. Regarding to the mentioned problems, the application of classifiers which are only based on the specific pixel intensity are subjected to the considerable failure [10]. Many methods have been presented for BMS [11]-[18]. BMS is classified to three main categories of boundary-based methods, region-based methods and hybrid methods [13], [14], [19], [20]. The gradient features near to an object boundary would be employed as a guide for segmentation in boundary-based strategies [21]. The main categories of this method are Edge detection, deformable templates and active contours [22-24]. The BMS in region-based methods is normally carried out with identification of homogenous region at corresponding brain tissues [25]. Hybrid approaches attempt to combine the strengths of both boundary-based and region-based approaches. On the other hand, BMS can be categorized as fuzzy and non-fuzzy strategies. In non-fuzzy classification-based methods, standard classifiers such as Gaussian mixture model, K-Means, KNN, and etc are used [26]. Basically, Brain extraction- operations and intensity non-uniformity correction are used to achieve desirable segmentation results [27]. Intensity uncertainty of brain MRI pixels encourages the researchers to develop fuzzy approaches, where different regions of the image are considered as fuzzy sets in which a pixel may be assigned to the potential multi-class tissues. Fuzzy segmentation methods offer more flexibility in classification of pixels with the same intensity than the other crisp methods [14]. A local fuzzy approach was presented at [28] which is needless of bias field estimation. A fuzzy rules-based segmentation strategy has been proposed in [29] based on anatomy knowledge. Fuzzy inference system is used to identify white matter tissue for elderly in [30]. Handcraft fuzzy rules which are presented for tissue classification at [31]. Unsupervised BMS has been presented in [32] based on fuzzy frame and tissue analysis. Fuzzy C-Mean (FCM) is one of the prominent tools among different fuzzy approaches in BMS [10], [14], [16], [33-35]. Different researches have been performed for FCM optimization with promising results. An adaptive FCM approach has been suggested in [36] to estimate INU with multiplying a distance function and clustering centers and this method is generalized for 3-D images in [37]. A regulative term has been used for proposed FCM in which the spatial information are interpreted to overcome noise effects [10].
In this paper, a fuzzy C-Mean with multi-dimensional objective function has been proposed for BMS. Feature extraction and selection have been carried out to achieve spatial information in order to overcome artifacts effect. The outline of the paper is as follows: In Section 2, basic concepts of fuzzy C-Means and Singular Value Decomposition (SVD) are introduced. Data bases and evaluation criteria are in section 3. Proposed method is explained in section 4. Simulation results are investigated in section 5 and the paper will be concluded at section 6.

2. BASIC CONCEPTS

2.1. Fuzzy c-Mean (FCM)

In FCM, as a development of hard K-means algorithm, every input data will be assigned to all the existing clusters [38]. Pattern membership of a class is based on the similarity of the pattern to the class with respect to all classes. The objective function of the FCM which segments an image to C clusters can be defined as

$$J_q(u,v)=\sum_{i=1}^{c}\sum_{j=1}^{n}u_{ij}^{q}d^2(x_j,v_i)$$
$$\text{subject to}\quad \sum_{i=1}^{c}u_{ij}=1 \quad \& \quad u_{ij}\in[0,1] \tag{1}$$

In which $\boldsymbol{X}=(x_1,x_2,\ldots,x_i,\ldots,x_n)$ is a $p\times n$ data matrix, p is the length of the feature vector $\boldsymbol{x}_j$and n is the number of feature vectors. In BMS, $p=1$ (intensity value), n is the number of image pixels, q is the fuzziness index (in this study, q is *2)*. u_{ij} is the membership of j^{th} pattern in i^{th} cluster, v_i is the center of i^{th} fuzzy cluster. d represents the similarity of the feature vector $\boldsymbol{x}_j$ with cluster center v_i in the feature space which can be calculated with the Euclidean norm as:

$$d^2(x_j,v_j)=\left\|x_j-v_j\right\|^2 \tag{2}$$

To minimize the objective function, higher membership values should be assigned to patterns which are close to cluster centers, and lower values assigned to patterns far from cluster centers. By applying derivation of J_q with respect to u and v, then setting this derivative equal to zero, the conditions to minimize the objectivation function (J_q) are:

$$u_{ij}=\left(\sum_{k=1}^{c}\left(\frac{d\left(x_j,v_i\right)}{d\left(x_j,v_k\right)}\right)^{2/(q-1)}\right)^{-1} \tag{3}$$

$$v_i=\frac{\sum_{j=1}^{n}u_{ij}^{q}x_j}{\sum_{j=1}^{n}u_{ij}^{q}} \tag{4}$$

According to Eq. 3 and 4, the patterns are assigned to all existing clusters with the associated Membership

Values (MVs), and then, the new cluster centers are calculated. The FCM algorithm reaches a solution by an iterative process until a termination criterion is met, ie. : $v(t)-v(t-1)<\varepsilon$. Finally, when the pattern to a cluster with the highest membership value is assigned, a segmentation of the data will be done.

2.2. Singular Value Decomposition (SVD)

Singular Value Decomposition (SVD) is one of the important tools used in digital signal and statistics data processing [39], [40]. Applying SVD on a typical $\boldsymbol{X}_{m\times n}$ matrix yields:

$$X = U\Sigma V^T \quad (5)$$

Where $\boldsymbol{U}_{m\times m}$ and $\boldsymbol{U}_{n\times n}$ are singular vector matrices and $\boldsymbol{\Sigma}_{m\times n}$ is a diagonal matrix with rank r. The diagonal entries of $\boldsymbol{\Sigma}$ ($\sigma_{11}>\sigma_{22}>\ldots>\sigma_{rr}>0$) are equal to the singular values of $\boldsymbol{X}$. In fact, these singular values contain some information about the signal energy. In a reconstruction process of $\boldsymbol{X}$, higher singular values are more effective.

3. MRI DATABASE AND EVALUATION CRITERIA

3.1. Brain MR Images

Simulated and manually segmented MR images play a key role for development of segmentation algorithm [41]. In this study, two publicly available datasets are used in which**,** the first one provided by Brainweb and the second one provided by the Internet Brain Segmentation Repository (IBSR).

3.1.1. Brainweb database

The Brainweb images are obtained from the brain database at the McConnell Brain Imaging Centre of the Montreal Neurological Institute (MNI), McGill University [42]. This database contains several acquisition modality (T1, T2, etc) and acquisition parameters. In this database, noise level varies between 0 to 9 percent and also, INU can be selected among one of 0, 20 or 40 percent.

3.1.2. IBSR datasets

IBSR provides real brain MRIs and the corresponding manual segmentation that are performed by the trained experts. The 20 normal MR brain datasets and their manual segmentations were provided by the Center for Morphometric Analysis at Massachusetts General Hospital [43]. In order to encourage the evaluation and development of segmentation algorithm.

3.2. Evaluation Criteria

Different criteria have been utilized in order to compare the proposed method with different strategies. These criteria are Accuracy (A), Dice similarity coefficient (D), also Known as Kappa statistics, and Tanimoto similarity coefficient (T) which are defined as follows:

$$A\% = \frac{TP+TN}{TP+TN+FP+FN}\times 100 \quad (6)$$

$$D\% = \frac{2\times TP}{(2\times TP)+FP+FN}\times 100 \quad (7)$$

$$T\% = \frac{TP}{TP+FP+FN}\times 100 \quad (8)$$

Where TP, TN, FP and FN are the numbers of true positive, true negative, false positive and false negative ones respectively [41], [44]. The greater the criteria, the better the segmentation.

4. PROPOSED METHOD

Spatial information is not considered in the objective function (J_m) of standard FCM. The main drawback of such a strategy in BMS has high sensitivity to noise pixels which leads to a considerable misclassification [14]. A substantial improvement can be achieved by using modified objective functions based on spatial information which results in a more robust results compared with the standard FCM [10], [14], [16], [33]-[35]. These methods employed modified objective functions considering pixel spatial information. In this study, a multi-dimensional FCM with a best feature combination capability has been utilized in order to consider spatial information. Fig. 2 shows a simple block diagram of proposed method.

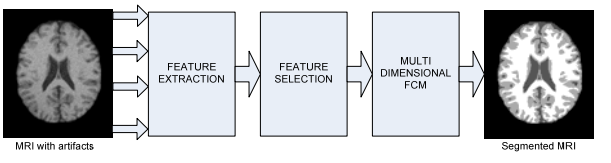

Fig.2. Block Diagram of the Proposed Method

This diagram includes: feature extraction, feature selection and multi dimensional standard FCM which can be described as follows:

4.1. Feature Extraction and Combination

The features considered in the analysis are: pixel intensity, mean, largest singular value and standard deviation of neighbourhood pixels. Mean, singular values and standard deviation (spatial information) are defined for each 3×3 matrix around the prototype pixel which is called L that's based on (9-11).

$$F_2 = \frac{\sum_{i=1}^{n} X_i}{n} = E(X) \quad (9)$$

Where x_i is the neighbourhood pixels value, $n=8$ is the number of neighbourhood pixels in each prototype pixel and $E(x)$ is mean or expected value. As mentioned

in section 2.2, The largest singular value can be calculated as:

$$SVD(L)=[U]\begin{bmatrix}\sigma_{11} & 0 & 0\\ 0 & \sigma_{22} & 0\\ 0 & 0 & \sigma_{33}\end{bmatrix}[V]^T \Rightarrow F_3=\sigma_{11} \quad (10)$$

σ_{11} is the largest singular value of L which contains significant information of the matrix and can be used as an important feature in BMS. F4 is calculated as:

$$F_4=\sqrt{\frac{\sum_{i=1}^{n}(X_i-E(x))^2}{n}} \quad (11)$$

It is clear that pixel intensity is the most important feature in BMS which contains precious information. Mean, standard deviation and the largest singular value features include information about neighbourhood pixels bias, discrepancy of neighbourhood pixels and the potency of crucial eigen-vector (see section 2.2) respectively. Possible combinations of the features are created to achieve the best feature set for BMS, which are as follows:

$$F_1,F_2,F_3,F_4,F_{12}=\begin{Bmatrix}F_1\\F_2\end{Bmatrix},F_{13}=\begin{Bmatrix}F_1\\F_3\end{Bmatrix},F_{14}=\begin{Bmatrix}F_1\\F_4\end{Bmatrix},$$

$$F_{123}=\begin{Bmatrix}F_1\\F_2\\F_3\end{Bmatrix},F_{134}=\begin{Bmatrix}F_1\\F_3\\F_4\end{Bmatrix},F_{124}=\begin{Bmatrix}F_1\\F_2\\F_4\end{Bmatrix},F_{1234}=\begin{Bmatrix}F_1\\F_2\\F_3\\F_4\end{Bmatrix} \quad (12)$$

As pixel intensity (F_1) contains more valuable information, it has to be available in all feature combinations. The best combination of features has to be selected from the available combination in feature selection stage. The number of features determines the FCM dimension ($P \geq 1$).

4.2. Feature Selection

For selecting the best combination of features, three slices of T1 weighted brain MRI of Brainweb database (z=60, 90, 120) are selected and the proposed algorithm have been implemented on the slices. Simulations are carried out in two categories in which the effects of noise and INU have been considered separately. Also Dice similarity and accuracy indexes are chosen for evaluation criteria.

4.2.1. Noisy Data

MRI slices with different noise levels have been segmented with proposed algorithm. The outputs of proposed segmentation algorithm have been compared by the ground truth and also the mean of accuracy and Dice similarity are shown in table 1 and 2 respectively. As highlighted in table 1 and 2, F_{134} is the best feature set that contains pixel intensity, singular value and standard deviation. Also, F_{14} (pixel intensity, standard deviation) shows an acceptable response. It is clear that standard deviation, itself, cannot be a proper feature with the noisy images and the algorithm does not have acceptable result. However, the significant point is that when this factor is combined with other features in a set, it leads to a suitable result. It means that the standard deviation contains potential information which is informative only in combination with other features.

Table1. Mean of Accuracy in different noise levels

	ALL	***CSF***	***GM***	***WM***
F_1	88.0	96.8	82.0	85.2
F_2	85.5	95.1	78.2	83.1
F_3	86.1	95.7	79.2	83.5
F_4	66.9	83.5	55.4	61.7
F_{12}	87.4	96.5	81.1	84.6
F_{13}	87.6	96.7	81.4	84.7
F_{14}	**88.1**	**95.9**	**82.2**	**86.3**
F_{123}	87.1	96.3	80.6	84.3
F_{124}	**88.1**	**96.3**	**82.2**	**85.9**
F_{134}	**88.4**	**96.6**	**82.5**	**85.9**
F_{1234}	87.8	96.4	81.7	85.3

Table 2. Mean of Dice Similarity in different noise levels

	ALL	***CSF***	***GM***	***WM***
F_1	89.9	90.9	89.0	89.8
F_2	89.6	89.1	89.1	90.8
F_3	90.5	90.1	90.0	91.4
F_4	48.7	43.5	49.8	52.8
F_{12}	91.9	92.1	91.4	92.2
F_{13}	91.9	92.1	91.4	92.2
F_{14}	88.6	89.2	87.6	89.2
F_{123}	91.7	91.6	91.3	92.2
F_{124}	92.3	92.0	91.9	93.0
F_{134}	**92.5**	**92.5**	**92.1**	**92.9**
F_{1234}	**92.6**	**92.4**	**92.3**	**93.2**

4.2.1. Data with INU

In this section, INU has been considered without noise. The outputs of proposed segmentation algorithm have been compared with the ground truth and the mean of accuracy and Dice similarity are shown in tables 3 and 4 respectively.

Table 3. Mean accuracy in different INU levels

	ALL	***CSF***	***GM***	***WM***
F_1	**95.9**	**98.2**	**93.9**	**95.8**
F_2	92.9	96.4	89.3	92.9
F_3	93.4	96.8	90.0	93.3
F_4	69.5	85.1	57.5	65.9
F_{12}	94.9	97.6	92.3	94.6
F_{13}	**95.0**	**97.8**	**92.6**	**94.8**

F_{14}	93.7	96.4	90.5	94.1
F_{123}	94.5	97.4	91.7	94.2
F_{124}	94.8	97.1	92.2	95.1
F_{134}	**95.0**	**97.3**	**92.5**	**95.2**
F_{1234}	**95.0**	**97.3**	**92.5**	**95.1**

Table 4. Mean Dice similarity in INU levels without noise

	ALL	*CSF*	*GM*	*WM*
F_1	**93.9**	**94.6**	**93.5**	**93.7**
F_2	89.2	89.3	88.5	89.8
F_3	90.0	90.3	89.3	90.3
F_4	53.0	48.9	51.6	58.4
F_{12}	92.3	93.1	91.8	92.1
F_{13}	92.3	92.4	92.0	92.4
F_{14}	90.4	90.3	89.9	91.1
F_{123}	91.7	92.4	91.1	91.6
F_{124}	92.1	92.0	91.7	92.5
F_{134}	**92.5**	**92.6**	**92.1**	**92.8**
F_{1234}	92.4	92.7	92.0	92.6

According to tables 3 and 4, pixel intensity is the best feature. It was expected that the use of neighbouring pixel's information cannot be beneficial due to absence of the noise.

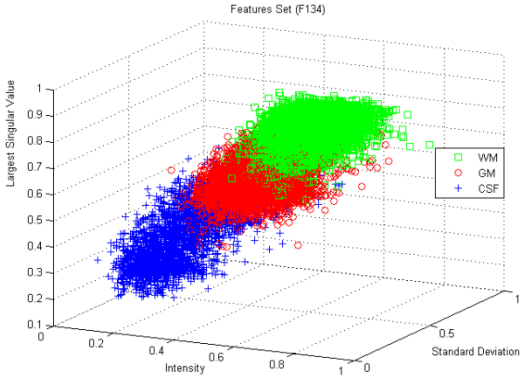

Fig. 3. 3D Tissues Overlapping of Fig. 1.(c)

Also, among the mentioned features combinations, F_{134} leads to better results. Based on the proposed results and also because of the fact that MRIs are subjected to noise and INU artifacts, a three dimensional FCM (3D FCM) with F_{134} feature set have been used as a classifier in the proposed method.3D selected features of Fig. 1 (c) are illustrated in Fig. 4.

5. RESULTS

The proposed algorithm is applied on two mentioned available databases. For such databases**,** extra non-brain tissues are removed before segmentation. Then, the proposed method will be compared with two different methods such as BCFCM [10] and LNLFCM [14] in 2D by Brainweb database and also it is compared with two state of the art methods in 3D. The first one of the state of the art method is NL-R-FCM [44] that is implemented on Brainweb database and the second one is CSWTSOM [41] which is implemented on IBSR database. In the BCFCM**,** all parameters are selected as reported in [10]. The parameters of LNLFCM are selected as: the standard deviation of the Gaussian Kernel is 30, the degree of filtering is 1000, window size of the neighborhood is 3 and the weights of all pixels in the window of searching are 7.

5.1. Simulated MR images

In this section, T1 weighted brain MRI from Brainweb database with slicethickness of 1 mm, volume size of 217×181×181 are employed to investigate the performance of the proposed method.

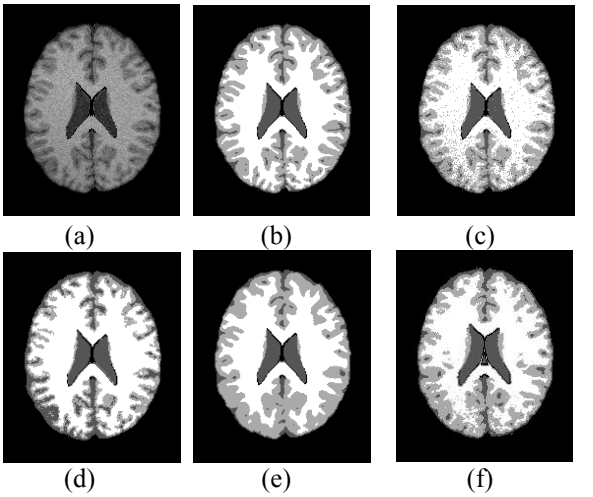

Fig. 4. Comparison of the segmentation results on a simulated brain MRI: (a) Original image with 9% noise and 40% INU (Slice = 94); (b) Ground truth; (c)FCM; (d)BCFCM; (e) LNLFCM and (f)Proposed method segmentation results

Fig. 4 (a) shows a slice of the simulated 3D volume of brain MRI with 9% Rician noiseand 40% INU (slice=96). The ground truth of this image is shown in the Fig. 4 (b). Segmentation results of BCFCM and LNLFCM are shown at Fig. 4 (c), (d) and (e), respectively. The result of the proposed method is shown in the Fig. 4 (f).

As shown in the Fig. 4 (c) we can visually see that the BCFCM are influenced by the artifact, intensively. It is worth mentioning that BCFCM is very sensitive to the selection of optimum parameters [10]. On the other hand, by comparison of the results shown in the Fig. 4 (d) and (b), it can be verified that the LNLFCM eliminate small piece of tissue with artifact effect elimination, so this problem decreases the performance

of such a technique. Dice similarity and Accuracy indexes of the Fig. 4 are shown in tables 5-6.

Table 5. Dice index for different methods in Fig. 4

	CSF	*GM*	*WM*
BCFCM	77.7	72.4	91.8
LNLFCM	89.0	88.2	93.2
Proposed	93.7	87.0	93.0

Table 6. Accuracy index for different methods in Fig. 4

	CSF	*GM*	*WM*
BCFCM	91.8	83.3	91.5
LNLFCM	96.8	91.0	93.3
Proposed	98.0	90.7	92.9

For more investigation of the performance of the proposed method, we implemented the proposed algorithmon 3D simulated brain MRI with 20% INU and various noise levels. The results of our method and NL-R-FCM are in table 7.

Table 7. Comparison of Dice similarity of the proposed method and NL-R-FCM applied on 3D simulated brain MRI with 20% INU and various noise levels

	WM		**GM**		**CSF**	
Method Noise	NL-R-FCM	Proposed	NL-R-FCM	Proposed	NL-R-FCM	Proposed
1%	94.7	94.8	94.1	92.7	---	92.7
3%	93.7	94.0	92.6	92.1	---	92.6
5%	92.0	92.9	89.6	91.1	---	92.5
7%	85.9	91.8	86.9	90.0	---	92.2
9%	83.4	88.7	83.5	87.0	87.3	90.9
Ave.	**90.0**	**92.5**	**89.3**	**90.6**	**---**	**92.2**

According to this table, by comparison of the proposed method with NL-R-FCM, it is emerges that our method leads to a satisfactory performance. Also this preference appears at 7% noise and above.

5.2. Real Brain MRI

In this section the proposed algorithm is evaluated for real brain MRI segmentation by IBSR database. Fig. 5 (a) and (b) show a slice of real T1-weighted normal MR image (IBSR 13_3, size of 256×256×56) and its manually segmented image as provided by the web respectively. Fig. 5 (c) shows the output of our proposed algorithm.

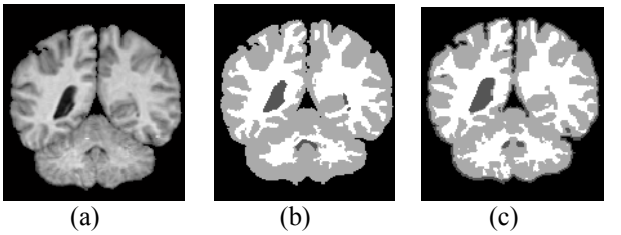

(a) (b) (c)

Fig. 5. T1-weighted real brain MRI (IBSR13-3, z=30): (a) original image; (b) manual segmentation; (c) our proposed algorithm segmentation result

Comparison of the Fig. 5 (c) with (b) shows the proposed frame that has good acceptable result. For quantitative evaluation purpose, the proposed methodimplemented on ten of twenty real normal MRIavailable data sets and the Dice and Tanimoto similarity coefficients are given in table 8. In this table, the results of CSWTSOM are given for comparison.

Table 8. Comparison of Dice and Tanimoto similarity coefficients of the proposed method and CSWTSOM applied on 3D real brain MRI

	Dice similarity						**Tanimotosimilarity**					
	WM			**GM**			**WM**			**GM**		
Dataset	CSWTSOM	Proposed		CSWTSOM	Proposed		CSWTSOM	Proposed		CSWTSOM	Proposed	
2_4	46.0	51.2		62.4	65.8		29.9	37.8		45.3	50.1	
5_8	72.1	66.7		81.7	76.7		56.4	49.9		69.1	62.8	
7_8	52.3	61.3		69.8	83.1		35.4	48.2		53.6	65.3	
11_3	77.3	80.9		82.2	83.2		62.3	62.6		69.8	70.2	
13_3	75.3	75.6		83.2	86.3		60.4	59.5		71.2	73.6	
16_3	71.3	73.5		81.7	76.2		55.4	60.6		69.1	65.6	
100_23	73.9	77.8		83.8	84.9		58.7	61.1		72.1	74.4	
111_2	79.1	80.2		80.1	84.1		65.4	66.1		67.8	70.8	
191_3	75.2	77.2		79.8	78.7		60.3	62.1		66.3	65.2	
205_3	77.6	77.1		82.7	82.3		63.3	63.3		70.5	70.1	
Average	**70.0**	**72.2**		**78.8**	**80.1**		**54.8**	**57.1**		**65.5**	**66.8**	

According to table 8, the 3DFCM shows acceptable results on 3D volume. Also it is obviously the average Dice and Tanimotosimilarity coefficients are better than CSWTSOM.

6. CONCLUSION

Spatial information is not considered in the objective function of standard FCM which leads to high sensitivity regarding to noise pixels and considerable misclassification. In this article, we proposed a multi dimensional FCM-based method for unsupervised brain MRI segmentation, by spatial information capturing in the features set. We show that the intensity, standard deviation and largest singular value are the best combination of extracted features. So, a 3DFCM is selected as proposed method. To verify the practical applicability of such a technique, simulations have been carried out on simulated and real datasets. The proposed method has been compared with BCFCM and LNLFCM in 2D comparison and also compared with NL-R-FCM and CSWTSOMalgorithms in 3D evaluation which shows a considerable improvement in brain MRI segmentation.

7. ACKNOWLEDGMENT

The authors are highly grateful to Jianzhong Wang and Dirk-Jan Kroonfor their kind support and helps. Also special thanks to BrainWeb Simulated Brain Database at the McConnell Brain Imaging Centre of the Montreal Neurological Institute (MNI), McGill University; and the Center for Morphometric Analysis at Massachusetts General Hospital (available at http://www.cma.mgh.harvard.edu/ibsr) for providing datasets.

REFERENCES

[1] C. R. G. Guttmann, F. A. Jolesz, R. Kikinis, R. J. Killiany, M. B. Moss, T. Sandor, and M. S. Albert, **"White matter changes with normal aging,"** *Neurology,* Vol. 50, pp. 972-78 April 1 1998.

[2] L. O'Donnell, **"Semi-Automatic Medical Image Segmentation,"** *Master of Science, Department of Electrical Engineering and Computer Science*, MASSACHUSETTS INSTITUTE OF TECHNOLOGY, MASSACHUSETTS, 2001.

[3] C. Brechbühler, G. Gerig, and G. Székely, **"Compensation of spatial inhomogeneity in MRI based on a multi-valued image model and a parametric bias estimate,"** In *Visualization In Biomedical Computing*, pp. 141-46, 1996.

[4] M. Styner, C. Brechbuhler, G. Szekely, and G. Gerig, **"Parametric estimate of intensity inhomogeneities applied to MRI,"** *IEEE transactions on medical imaging,* Vol. 19, pp. 153-65, Mar 2000.

[5] S. Prima, N. Ayache, T. Barrick, and N. Roberts, **"Maximum Likelihood Estimation of the Bias Field in MR Brain Images: Investigating Different Modelings of the Imaging Process,"** presented at the Proceedings of the 4th *International Conference on Medical Image Computing and Computer-Assisted Intervention, Utrecht*, The Netherlands, 2001.

[6] A. Montillo, J. K. Udupa, L. Axel, and D. Metaxas, **"Integrated approach for the removal of intensity inhomogeneity and thermal noise in SPAMM-MRI using scale-based fuzzy connectedness and multiple nonlinear adaptive filters,"** in *SPIE Medical Imaging*, 2003, pp. 1025–1036.

[7] A. Simmons, P. S. Tofts, G. J. Barker, and S. R. Arridge, **"Sources of intensity nonuniformity in spin echo images at 1.5 T,"** *Magnetic resonance in medicine : official journal of the Society of Magnetic Resonance in Medicine,* Vol. 32, pp. 121-8, Jul 1994.

[8] J. G. Sled, A. P. Zijdenbos, and A. C. Evans, **"A nonparametric method for automatic correction of intensity nonuniformity in MRI data,"** *IEEE transactions on medical imaging,* Vol. 17, pp. 87-97, Feb 1998.

[9] J. D. Gispert, S. Reig, J. Pascau, J. J. Vaquero, P. Garcia-Barreno, and M. Desco, **"Method for bias field correction of brain T1-weighted magnetic resonance images minimizing segmentation error,"** *Human brain mapping,* Vol. 22, pp. 133-44, Jun 2004.

[10] M. N. Ahmed, S. M. Yamany, N. Mohamed, A. A. Farag, and T. Moriarty, **"A modified fuzzy C-means algorithm for bias field estimation and segmentation of MRI data,"** *IEEE transactions on medical imaging,* Vol. 21, pp. 193-9, Mar 2002.

[11] D. L. Pham, C. Xu, and J. L. Prince, **"A survey of current methods in medical image segmentation,"** *Annual Review of Biomedical Engineering,* Vol. 2, pp. 315-337, 2000.

[12] A. Liew and H. Yan, **"Current Methods in the Automatic Tissue Segmentation of 3D Magnetic Resonance Brain Images,"** *Current Medical Imaging Reviews,* Vol. 2, pp. 91-103, 2006.

[13] W. J. Niessen, K. L. Vincken, J. Weickert, B. M. T. H. Romeny, and M. A. Viergever, **"Multiscale Segmentation of Three-Dimensional MR Brain Images,"** *International Journal of Computer Vision,* Vol. 31, pp. 185-202, 1999.

[14] J. Wang, J. Kong, Y. Lu, M. Qi, and B. Zhang, **"A modified FCM algorithm for MRI brain image segmentation using both local and non-local spatial constraints,"** *Computerized medical imaging and graphics : the official journal of the Computerized Medical Imaging Society,* Vol. 32, pp. 685-98, Dec 2008.

[15] S. B. Mehta, S. Chaudhury, A. Bhattacharyya, and A. Jena, **"A soft-segmentation visualization scheme for magnetic resonance images,"** *Magnetic Resonance Imaging,* Vol. 23, pp. 817-828, 2005.

[16] Z.-X. Ji, Q.-S. Sun, and D.-S. Xia, **"A modified possibilistic fuzzy c-means clustering algorithm for bias field estimation and segmentation of brain MR image,"** *Computerized Medical Imaging and Graphics,* Vol. 35, pp. 383-397, 2011.

[17] Z. Zhou and Z. Ruan, **"Multicontext wavelet-based thresholding segmentation of brain tissues in magnetic resonance images,"** *Magnetic Resonance Imaging,* Vol. 25, pp. 381-385, 2007.

[18] Z. Y. Shan, J. Z. Liu, and G. H. Yue, **"Automated human frontal lobe identification in MR images based on fuzzy-logic encoded expert anatomic knowledge,"** *Magnetic Resonance Imaging,* Vol. 22, pp. 607-617, 2004.

[19] Y. Zhuge, J. K. Udupa, and P. K. Saha, **"Vectorial scale-based fuzzy-connected image segmentation,"** *Computer Vision and Image Understanding,* Vol. 101, pp. 177-193, 2006.

[20] K. C. Ciesielski, J. K. Udupa, P. K. Saha, and Y. Zhuge, **"Iterative relative fuzzy connectedness for multiple objects with multiple seeds,"** *Computer Vision and Image Understanding,* Vol. 107, pp. 160-182, 2007.

[21] M. Bomans, K. H. Hohne, U. Tiede, and M. Riemer, **"3-D segmentation of MR images of the head for 3-D display,"** *IEEE transactions on medical imaging,* Vol. 9, pp. 177-83, 1990.

[22] T. McInerney and D. Terzopoulos, **"Deformable models in medical image analysis: a survey,"** *Medical image analysis,* Vol. 1, pp. 91-108, Jun 1996.

[23] L. Ji and H. Yan, **"An attractable snakes based on the greedy algorithm for contour extraction,"** *Pattern Recognition,* Vol. 35, pp. 791-806, 2002.

[24] W. Abd-Almageed, A. El-Osery, and C. Smith, **"A fuzzy-statistical contour model for MRI segmentation and target tracking,"** presented at the SPIE, Orlando, FL, USA 2004.

[25] T. Heinonen, P. Dastidar, H. Eskola, H. Frey, P. Ryymin, and E. Laasonen, **"Applicability of semi-automatic segmentation for volumetric analysis of brain lesions,"** *Journal of medical engineering & technology,* Vol. 22, pp. 173-8, Jul-Aug 1998.

[26] R. O. Duda, P. E. Hart, and D. G. Stork, **"Pattern Classification,"** ed: John Wiley & Sons Inc, 2001.

[27] U. Vovk, F. Pernus, and B. Likar, **"A review of methods for correction of intensity inhomogeneity in MRI,"** *IEEE transactions on medical imaging,* Vol. 26, pp. 405-21, Mar 2007.

[28] C. Zhu and T. Jiang, **"Multicontext fuzzy clustering for separation of brain tissues in magnetic resonance images,"** *NeuroImage,* Vol. 18, pp. 685-96, Mar 2003.

[29] G. R. Hillman, C.-W. Chang, H. Ying, J. Yen, L. Ketonen, and T. A. Kent, **"A Fuzzy Logic Approach to Identifying Brain Structures in MRI Using Expert Anatomic Knowledge,"** *Computers and Biomedical Research,* Vol. 32, pp. 503-516, 1999.

[30] F. Admiraal-Behloul, D. M. van den Heuvel, H. Olofsen, M. J. van Osch, J. van der Grond, M. A. van Buchem, and J. H. Reiber, **"Fully automatic segmentation of white matter hyperintensities in MR images of the elderly,"** *NeuroImage,* Vol. 28, pp. 607-17, Nov 15 2005.

[31] S. B. Mehta, S. Chaudhury, A. Bhattacharyya, and A. Jena, **"Handcrafted fuzzy rules for tissue classification,"** *Magnetic Resonance Imaging,* Vol. 26, pp. 815-823, 2008.

[32] G. Wiselin and G. Wiselin Jiji, **"Unsupervised Segmentation using Fuzzy Logic based Texture Spectrum for MRI Brain Images,"** presented at the Third World Enformatika Conference, WEC'05, Istanbul, Turkey, 2005.

[33] K. S. Chuang, H. L. Tzeng, S. Chen, J. Wu, and T. J. Chen, **"Fuzzy c-means clustering with spatial information for image segmentation,"** *Computerized medical imaging and graphics : the official journal of the Computerized Medical Imaging Society,* Vol. 30, pp. 9-15, Jan 2006.

[34] A. W. Liew and H. Yan, **"An adaptive spatial fuzzy clustering algorithm for 3-D MR image segmentation,"** *IEEE transactions on medical imaging,* Vol. 22, pp. 1063-75, Sep 2003.

[35] S. Ramathilagam, R. Pandiyarajan, A. Sathya, R. Devi, and S. R. Kannan, **"Modified fuzzy c-means algorithm for segmentation of T1-T2-weighted brain MRI,"** *Journal of Computational and Applied Mathematics,* Vol. 235, pp. 1578-1586, 2011.

[36] D. L. Pham and J. L. Prince, **"An adaptive fuzzy C-means algorithm for image segmentation in the presence of intensity inhomogeneities,"** *Pattern Recognition Letters,* Vol. 20, pp. 57-68, 1999.

[37] D. L. Pham and J. L. Prince, **"Adaptive fuzzy segmentation of magnetic resonance images,"** *IEEE transactions on medical imaging,* Vol. 18, pp. 737-52, Sep 1999.

[38] J. C. Bezdek, *Pattern recognition with fuzzy objective function algorithms*. New York ; London: Plenum, 1981.

[39] J. Ghasemi and M. R. K. mollaei, **"A New Approach for Speech Enhancement Based On Eigenvalue Spectral Subtraction,"** *Signal Processing : An International Journal,* Vol. 3, pp. 34-41, 2009.

[40] A. Afzalian, M. R. K. Mollaei, M. Dousti, and J. Ghasemi, **"A New Approach for Speech Enhancement Based On Singular Value Decomposition and Wavelet Transform,"** *Australian Journal of Basic and Applied Sciences,* Vol. 4, pp. 3602-12, August, 2010.

[41] A. Demirhan and I. Güler, **"Combining stationary wavelet transform and self-organizing maps for brain MR image segmentation,"** *Engineering Applications of Artificial Intelligence,* Vol. 24, pp. 358-367, 2011.

[42] Available: http://www.bic.mni.mcgill.ca/brainweb.

[43] Available: http://www.cma.mgh.harvard.edu/ibsr.

[44] B. Caldairou, N. Passat, P. A. Habas, C. Studholme, and F. Rousseau, **"A non-local fuzzy segmentation method: Application to brain MRI,"** *Pattern Recognition,* Vol. 44, pp. 1916-1927, 2011.